Brain Advance Access published May 13, 2011

BRAIN
A JOURNAL OF NEUROLOGY

Examining working memory task acquisition in a disrupted neural network

Frank G. Hillary,[1,2] John D. Medaglia,[1] Kathleen Gates,[3] Peter C. Molenaar,[3] Julia Slocomb,[2] Alyssa Peechatka[1] and David C. Good[2]

1 Department of Psychology, Pennsylvania State University, University Park, PA 16801, USA
2 Department of Neurology, Hershey Medical Centre, Hershey, PA 16801, USA
3 Department of Human Development and Family Sciences, University Park, PA 17033, USA

Correspondence to: Frank G. Hillary, PhD,
Department of Psychology,
Pennsylvania State University,
223 Bruce V. Moore Building,
University Park, PA 16802,
USA
E-mail: fhillary@psu.edu

There is mounting literature that examines brain activation during tasks of working memory in individuals with neurological disorders such as traumatic brain injury. These studies represent a foundation for understanding the functional brain changes that occur after moderate and severe traumatic brain injury, but the focus on topographical brain-'activation' differences ignores potential alterations in how nodes communicate within a distributed neural network. The present study makes use of the most recently developed connectivity modelling (extended-unified structural equation model) to examine performance during a well-established working-memory task (the *n*-back) in individuals sustaining moderate and severe traumatic brain injury. The goal is to use the findings observed in topographical activation analysis as the basis for second-level effective connectivity modelling. Findings reveal important between-group differences in within-hemisphere connectivity during task acquisition, with the control sample demonstrating rapid within-left hemisphere connectivity increases and the traumatic brain injury sample demonstrating consistently elevated within-right hemisphere connectivity. These findings also point to important maturational effects from 'early' to 'late' during task performance, including diminished right prefrontal cortex involvement and an anterior to posterior shift in connectivity with increased task exposure. We anticipate that this approach to functional imaging data analysis represents an important future direction for understanding how neural plasticity is expressed in brain disorders.

Keywords: brain injury; brain plasticity; connectivity; structural equation model; working memory
Abbreviations: BOLD = blood oxygen level-dependent; TBI = traumatic brain injury

Introduction

Traumatic brain injury (TBI) is the most common neurological disorder in the USA, with a lifetime prevalence recently determined to be 2% (Langlois *et al*., 2004). In moderate and severe cases, the frontal lobes are affected ~70% of the time (Hillary *et al*., 2001; Hart *et al*., 2005) and, because of this, research has consistently focused on frontal systems that regulate attention, processing efficiency and working memory (or the ability to maintain a small amount of information 'in mind' for online manipulation).

Over the past decade, the field of clinical neuroscience has seen a dramatic increase in the use of advanced neuroimaging

Received September 28, 2010. Revised December 20, 2010. Accepted January 21, 2011.

techniques to examine cognitive, sensory and motor dysfunction in individuals with neurological impairment. One rapidly growing body of literature has examined alterations in basic information processing after moderate and severe TBI, including examination of executive control (Scheibel *et al*., 2007, 2009; Turner and Levine 2008), processing speed (Hillary *et al*., 2010), memory encoding (Ricker *et al*., 2001; Levine *et al*., 2002; Strangman *et al*., 2009) and working memory (Christodoulou *et al*., 2001; Perlstein *et al*., 2004; Maruishi *et al*., 2007; Newsome *et al*., 2007; Sanchez-Carrion *et al*., 2008*a, b*). These studies provide the foundation for understanding the large-scale functional brain changes occurring after moderate and severe TBI in adults. For example, in imaging studies of working memory, one finding that occurs almost universally after TBI is the recruitment of regions in the prefrontal cortex (and often right prefrontal cortex, specifically) and anterior cingulate cortex (for reviews see Hillary *et al*., 2006; Hillary 2008).

What remains unclear in this literature is the nature of prefrontal cortex/anterior cingulate cortex recruitment and how it supports (or possibly inhibits) recovery of function. In a series of papers, we proposed and tested the 'latent resource hypothesis', which maintains that neural recruitment after TBI is not abberant or formal 'reorganization', but instead represents the natural waxing and waning of executive control during variable cerebral challenge (Hillary *et al*., 2006, 2010; Hillary, 2008). As an extension of this position, we proposed that right prefrontal cortex is differentially recruited in neurological samples because of the role the right hemisphere has been shown to play in handling novel task demands (Pardo *et al*., 1991). In the current study, this conceptualization of neural recruitment after injury provides a framework for testing hypotheses about how disrupted neural systems implement novel tasks.

To date, studies that examine functional brain activation differences after TBI have focused almost exclusively on documenting the brain regions where the blood oxygen level-dependent signal (BOLD) differentiates the groups topographically. This approach has been the methodological standard in the clinical neurosciences using functional MRI to understand plasticity following neurological compromise; but focus on the between-group differences in brain topography offers little information regarding how components within neural networks interact following neural disruption. For example, measurement of activation topography ignores the critical possibility that even equivalent results between groups may disguise very important differences in network functioning—differences that are observable only when determining how the components within the network communicate. Thus, while neural recruitment has emerged as the most common finding in studies examining the magnitude of the BOLD signal change (i.e. activation), there are no studies to date using effective connectivity modelling to examine how the neural recruitment repeatedly observed after TBI has bearing on network communication.

Critical early work in neural network modelling occurred over a decade ago (McIntosh and Gonzalez-Lima, 1994) and there have been important advancements in modelling of time series brain data since that time (Friston *et al*., 1994, 1995; Kim *et al*., 2007; Oikonomou *et al*., 2010). For example, in one application of network modelling, investigators demonstrated altered connectivity in a case of amnesia (Maguire *et al*., 2001). Overall, however, the use of effective connectivity to understand the consequences associated with neurological disorder has been sparse. If we were to extend the latent resource hypothesis to effective connectivity modelling, we might anticipate that prefrontal cortex (and often right prefrontal cortex) should be differentially involved in tasks of working memory (or other tasks requiring cognitive control engagement) in patients with TBI compared to healthy controls. This position also maintains that, with increased task facility, the response in prefrontal cortex of individuals with TBI should reflect similar downregulation of prefrontal cortex as demand on excutive control diminishes. If this characterization of prefrontal cortex recruitment in TBI is accurate, individuals sustaining injury should demonstrate greater right prefrontal cortex connectivity compared to healthy controls, but with continued exposure to a new task, this influence should diminish as task proceduralization occurs, thus resulting in reduced demand on anterior portions of the network overall. In the current study, we use the most advanced connectivity modelling available to examine this conceptualization of prefrontal cortex recruitment after neurological disruption.

In a recent study examining resting-state connectivity after TBI, Nakamura *et al.* (2009) applied graph-theory analysis to examine whole-brain 'small-worldness' during recovery, documenting changes in resting state connectivity during the first 6 months following injury. Recovery from injury revealed greater clustering of connections, greater 'small-worldness' and a reduction in the overall number of highly significant connections. The resting state connectivity findings in Nakamura *et al.* (2009) included an extensive number of regions of interest, but the direction of network connectedness during recovery may offer important information about what is to be expected in the current sample. For example, we anticipate that, compared to a TBI sample, a healthy control sample would exhibit a sparser network, but the TBI sample would demonstrate convergence toward a parsimonious network with increased task exposure.

Thus, the goal of this study is to use recently advanced connectivity modelling to examine a well-established working memory task in a group of individuals with TBI. Of importance here, the topographical activation results are known and consistent with a larger literature (e.g. prefrontal cortex recruitment in TBI), thus permitting direct examination of network connectivity in TBI where neural recruitment has been observed. In doing so, this is the first study to use advanced connectivity modelling to examine new learning following neurological compromise.

Study hypotheses

Given the clinical heterogeneity inherent in TBI, one aim of the current study was to focus on within-subject change in order to determine how networks are altered with task exposure. To do so, we examined effective connectivity during early trials, comparing these early models with later connectivity models after greater facility has been developed within the task (henceforth, referred to as 'early' and 'late' task effects). Based upon prior cross-sectional topographical activation studies in this literature and

our recent findings in TBI, there are three hypotheses regarding effective connectivity after moderate and severe TBI.

Hypothesis 1a

Based on the latent resource hypothesis and the postulated role of the right hemisphere in handling task novelty during acquisition, we anticipate that, during early task exposure, individuals with TBI will demonstrate greater right hemisphere connectivity within the network compared to healthy adults.

Hypothesis 1b

Related to Hypothesis 1a, we anticipate that with increased exposure to a novel task, right hemisphere (and specifically right prefrontal cortex) influence on the network will diminish over time.

Hypothesis 2

Based on our prior work, examining resting connectivity in TBI (Nakamura *et al*., 2009), we anticipate that individuals with TBI will demonstrate a greater total number of overall connections and greater inter-hemispheric connectivity compared to healthy controls and that these should diminish with increased task efficiency.

Hypothesis 3

As an exploratory hypothesis, we anticipate that with prolonged task exposure and increased task efficiency, network modulation will result in reduced anterior influence (e.g. due to reduced demand in cognitive control) and therefore relatively greater posterior influence (e.g. due to formalized sensory representation).

Materials and methods

Subjects

Participants included 12 right-handed individuals with moderate and severe TBI and 12 right-handed matched healthy controls between the ages of 18 and 53 years without any reported medical or psychiatric disabilities. Demographic and clinical characteristics of the sample are presented in Table 1. TBI severity was defined using the Glasgow Coma Scale in the first 24 h after injury (Teasdale and Jennett, 1974). Glasgow Coma Scale scores from 3 to 8 were considered 'severe' and scores from 9 to 12, or individuals with significant neuroimaging findings, were considered 'moderate'. All individuals with TBI had an initial Glasgow Coma Scale score of 3–12 and/or had at least one identifiable brain lesion site as confirmed by acute neuroimaging reported in their medical records. Candidates for the study were excluded if they had a history of neurological disorder such as prior TBI, stroke or seizure disorder or significant neuro-developmental psychiatric history (such as schizophrenia or bipolar disorder). Individuals were also excluded if they had a history of inpatient treatment for substance abuse. These exclusions were assessed via medical chart review and were covered in the institutional review board-approved consent form and were discussed/confirmed with the study participant and/or the family member(s) of each participant at the time of study enrolment.

Magnetic resonance imaging

A visual sequential letter task, the *n*-back, was used to assess working memory. Alphabetical letters were presented at a rate of one every 2 s (stimulus duration = 1750 ms, interstimulus interval = 250 ms). The subjects were instructed to press a response button as quickly as possible whenever the current letter was the same as the letter immediately preceding it (1-back task) or two letters prior (2-back task; Speck *et al*., 2000; Chang *et al*., 2001). The current block design alternated between 20 s 'on' and 14 s 'off' blocks. During each 20 s block, three or four positive targets (i.e. 'yes' responses) were presented at pseudo-random intervals and a total of 21–24 targets were presented per run for a total of 80 stimuli per run. During the rest period (14 s), subjects were instructed to fixate on a small asterisk presented at the centre of the display screen. As part of a larger study examining task practice, after initial MRI scanning, subjects were removed from the MRI environment and permitted to rest briefly (~5 min) and then proceeded to practice outside of the scanner one run of 1-back and one run of 2-back tasks before returning to the MRI environment. For the purposes of the current connectivity analysis, we focus here on the initial MRI session only (a single extended 1-back and 2-back per subject).

All data were acquired using a Philips 3 T system and a 6-channel SENSE head coil (Philips Medical Systems, Best). First, 3D high-resolution T_1-weighted magnetization-prepared rapid acquisition with gradient echo (MPRAGE) images (9.9 ms/4.6 ms/8° repetition time/echo time/flip angle, $240 \times 204 \times 150\,mm^3$ field of view, $256 \times 205 \times 150$ acquisition matrix, two averages) were acquired to provide high resolution underlays for functional brain activation. Echo planar imaging was used for functional imaging. Imaging parameters consisted of: 2000 ms/30 ms/89°, repetition time/echo time/flip angle, $230 \times 230\,mm^2$ field of view, 80×80 acquisition matrix, 344-mm-thick axial slices with no gap between slices.

Data preprocessing

Preprocessing of the functional MRI data was performed using SPM 5 software (http://www.fil.ion.ucl.ac.uk/spm5). The first nine volumes were removed from analyses in order to control for initial signal instability. Pre-processing steps included realignment of functional data of each trial to the first functional image of that trial using affine transformation (Worsley and Poline, 1995; Ashburner and Friston, 1997). Functional images were then co-registered to the individual's T_1 magnetization prepared rapid gradient echo and all data were normalized using a standardized T_1 template from the Montreal Neurological Institute, using a 12-parameter affine approach and bilinear interpolation. Normalized time series data were smoothed with a Gaussian kernel of $8 \times 8 \times 10\,mm^3$ in order to minimize anatomical differences and increase signal to noise ratio.

Functional imaging contrasts

First level analyses using the general linear model within SPM5 produced intra-individual 2-back minus rest and 1-back minus rest contrasts. These contrasts were used to guide region of interest determination (see below). Topographical activation results from between-group analysis is available in Medaglia *et al*. (manuscript under review), but in brief, individuals with TBI demonstrated greater activation in working-memory networks compared to healthy controls during the 1-back task and slower reaction times and comparable activation and performance compared to the healthy controls during

Table 1 Demographic results for traumatic brain injury and healthy control samples and clinical descriptors for traumatic brain injury sample

Demographic variables					
			TBI, mean (SD)	Healthy controls, mean (SD)	Group comparison, *P*-value
Age			32.17 (12.23)	25.08 (10.24)	0.13
Education			13.75 (2.60)	14.08 (1.93)	0.79
Gender					
Male			6	7	0.68
Female			6	5	

TBI sample number	Glasgow Coma Scale	Years post injury	Acute care (days)	LOC (days)	CT/MRI finding
1	3	1.9	7	4	Subarachnoid haemorrhage within quadrigeminal cistern and occipital horns of lateral ventricles bilaterally; diffuse axonal injury in right frontal and parietal lobes and in left caudate head
2	7	7.8	21	14	Diffuse axonal injury, frontal lobe and cerebellum
3	3	1.9	16	15	Right frontal haemorrhage; small subdural haemorrhage; subdural haematoma; intraventricular haemorrhage; focal parenchymal haemorrhage in bilateral frontoparietal lobe, right inferior frontal lobe, left basal ganglia
4	3	18.8	37	14	Lesion to left motor strip white matter, small focal lesion in deep left frontal white matter; epidural haematoma
5	3	2.8	24	21	Bilateral subdural haematoma (larger on left than right); mild shift, intraparenchymal haemorrhage in left frontoparietal lobe; oedema and effacements; left sylvian fissure and basal cisterns
6	3	12.1	22	11	Right frontal and parietal epidural haematoma; left parietal subdural haematoma; diffuse subarachnoid haemorrhage: left to right shift, diffuse oedema, left temporal lobe parenchymal haematomas
7	3	14.7	11	8	Mid-brain, diffuse axonal injury; left thalamus, mid-cerebellar and brainstem atrophy
8	3	3.6	13	2–3	Frontal petechial haemorrhages, right frontal lobe and right temporal horn, putamen, and right parasagittal cortex; diffuse axonal injury in right thalamus (largest); haemorrhage in ventricles and along the left tentorium and right mesotemporal lesions
9	7	6.6	9	11	Left temporoparietal parenchymal haemorrhage; intraparenchymal haemorrhage in left posteroparietal region; small subdural haematoma bilaterally
10	3	5.7	32	Unknown	Bilateral intraventricular haemorrhage and intraparenchymal haemorrhage throughout parietal and frontal lobes
11	Unknown	5.2	6	1	High right parieto-occipital subdural haematoma/epidural haematoma
12	4	21.3	24	7	Haemorrhage in lateral, third and fourth ventricles, more prominent in left lateral ventricle; haemorrhage contusion in left thalamus; subgaleal haematoma in left temporoparietal lobe
Mean (SD)	3.8 (1.6)	8.5 (6.6)	18.5 (9.9)	10.6 (5.8)	

LOC = loss of consciousness; TBI = traumatic brain injury.

the 2-back task. Both groups recruited additional neural resources to successfully engage in the 2-back compared to the 1-back. Finally, over time (early versus late trials), both groups demonstrated reduced prefrontal cortex involvement with prolonged task exposure. These data are largely consistent with prior studies examining working-memory performance in TBI, affording the opportunity to examine the implications these findings have for effective connectivity networks.

Creating region of interest time series for connectivity analysis

To arrive at connectivity models, original region of interest time series data were collected based upon peak and surrounding activation in six predetermined Brodmann areas chosen based on substrates demonstrated in the working memory literature to be recruited after TBI.

These regions are bilateral frontal (Brodmann area 46), anterior cingulate (Brodmann area 32) and parietal (Brodmann area 40) regions subserving working memory functioning (Hillary, 2008). Activation was determined by locating the peak voxel and, based on this voxel, a mean-centred time series of BOLD signal intensity over the course of the time series was extracted for the identified peak voxel and a corresponding 5 mm radius sphere surrounding the peak for each Brodmann area using the MarsBar toolbox in SPM 5. Each identified peak voxel was examined against the Talairach Daemon after conversion to Talairach space (Brett, 1999) in order to guarantee that it was spatially located within the Brodmann area of interest. Of note, we used a 'thresholding to inclusion' procedure to guarantee that all subjects had a 'peak' in each of the six regions of interest. To do so, the threshold for determining peak activation was initially constrained at $P < 0.001$ uncorrected to locate the highest peak within each of the six Brodmann areas. When this threshold revealed no appropriate peaks in a Brodmann area, the threshold was relaxed to a maximum of $P < 0.25$. In the rare case that peak activation was apparent; an adjacent region of interest also linked to similar working-memory function was permitted (e.g. Brodmann areas 32/24, 46/9, 40/39). While this threshold might be problematic in the study of regional mean signal change (i.e. studies of activation), it is justified here with the understanding that regions of interest with weaker mean signal change at this first step would not influence connectivity results (i.e. regions of interest truly uninvolved in task do not demonstrate systematic covariance with those involved in task). Thus, we used liberal thresholding at this first step to include subject-specific BOLD connectivity for every region of interest and then permitted the second step, which included very stringent criteria, to prune any spurious connections. Then, for each subject the time-series for all six regions of interest were submitted to secondary (i.e. connectivity) analysis. Connectivity data are based on the relationships between mean signal intensities for each spherical region of interest along the time-series, including during and in the absence of task stimulation. The influence of task onsets on mean signal in regions of interest was modelled explicitly with other vectors of interest during connectivity modelling (see description below).

Connectivity analysis: the extended-unified structural equation model

Based on the selection of the six regions of interest determined with the procedure outlined above, connectivity between these six nodes (i.e. bilateral frontal, anterior cingulate and parietal regions) was determined by using extended-unified structural equation modelling. For a detailed description of the extended-unified structural equation model and its validation, please refer to recent work by Gates *et al.* (2010*a, b*). The extended unified structural equation model maintains several important advantages over previously developed algorithms. First, it offers the opportunity to examine both contemporaneous and lagged effects for all nodes within the model simultaneously that reduces biases occurring in modelling when these effects are not considered, such as in vector auto-regression and traditional structural equation modelling (Kim *et al*., 2007; Gates *et al*.,2010*a*). The extended unified structural equation model explicitly models the modulating effects of input on the relationships between regions of interest *via* bilinear terms that consider the hemodynamic response function plus an error term, thus affording a stochastic (or non-deterministic) approach to neural modelling. For the purposes of this study, perhaps the most important advancement offered by the extended unified structural equation model is that it permits both confirmatory and exploratory data analyses, thus allowing for a data-driven approach to hypothesis testing. In summary, extended unified structural equation model modelling for a single input (i.e. task) and 'lag' (i.e. prior voxel status predicts later voxel status) of one can be captured as:

$$\eta_t = \underbrace{A\eta_t}_{\text{Cont.}} + \underbrace{\phi_1 1\eta_{t-1}}_{\text{Lagged}} + \underbrace{\gamma_0 u_t + \gamma_1 u_{t-1}}_{\text{Input}} + \underbrace{\tau_{11}\eta_{t-1}u_{t-1}}_{\text{Modulating}} + \varsigma_t$$

The extended unified structural equation model, where η indicates the region of interest time series, u a one-vector input series (which may be expanded to include more inputs) convolved with a haemodynamic response function (Sarty, 2006), A the contemporaneous relations among regions of interest, Φ the lagged associations, γ input effects, τ the bilinear associations and ζ error assumed to be a white noise process. Note that this equation applies specifically to a lag of one. For a more general model of q-order time lags refer to Kim *et al*. (2007).

Application of the extended unified structural equation model: rationale and procedure

Rationale

One primary concern when conducting connectivity analyses is the potential for generating connectivity maps at the group level that fail to describe any one individual in the group. Current approaches for aggregating across individuals all suffer from this potential pitfall because they assume ergodicity, or similar patterns, across subjects. However, it is reasonable to assume that there may be more than one way in which spatial integration occurs in any group member. For example, if there were just two different network patterns in a group of subjects (which is a very conservative estimate for working memory), previous structural equation model algorithms for concatenating time series aim to accommodate the two patterns, arriving at estimated parameters for all connections that are seen across the individuals. In the process, however, a map emerges that often explains no one person and with the high probability of containing spurious connections not observed in any individual group member (Gates *et al.*, 2010*b*). In this case, the group model presents information that falsely informs investigators about the true state of the neural system. For these reasons, we focus on extended unified structural equation model analysis applied at the individual level and from these estimates we can examine between-group differences and network change over time using estimates we are assured describe the individual network processes.

Procedure

Covariance matrices were created of each half of the individual's region of interest time series for the 1-back and 2-back conditions. This resulted in four matrices representing 'early' and 'late' for each n-back condition per person. The covariance matrices used for connectivity analysis was 20×20 and included: six region of interest time series at time t (where t ranges across the sequence of registrations); the same six region of interest time series at the next time $t+1$ (lagged series); two time series of the direct effects of the input convolved with the same canonical haemodynamic response function used to determine region of interest activation (at time t and lagged at the next time $t+1$); and six bilinear series representing the region of interest time series at each time t multiplied with the convolved input series at time t. The automatic extended-unified structural equation model search (cf. Gates*et al*., 2010*a*) was applied to each matrix.

Model fit parameters found to demonstrate reliability in simulation studies (cf. Gates *et al*., 2010) were chosen *a priori* so that all of the following were maintained in the final model derived from the automatic search: root mean squared error of approximation <0.05; standardized root mean squared residual <0.05; non-normed fit index >0.95, and the comparative fit index $= 0.95$. This procedure offers a conservative estimate of connection β-values that are less sensitive to sample size and number of parameters (Brown, 2006). Once the appropriate model was identified, all non-significant individual β-parameters were trimmed (Gates *et al*., 2010*b*), and the final pattern of β-parameters was submitted to a confirmatory model to obtain the best estimates that would be expected if the study were replicated for that person.

For the purposes of this article, only contemporaneous effects are tested and presented in second-level analyses. One reason for this is that because the resolution in functional MRI is much cruder than the millisecond scale of actual neural events, lagged effects are difficult to interpret. These analyses do, however, account for the influence of time-lagged effects on effective connectivity, resulting in unbiased estimates of contemporaneous effective connectivity.

Neuropsychological testing

On the same day as MRI scanning, a battery of neuropsychological tests was administered to each participant to assess cognitive function. The battery assessed common cognitive functions known to be impaired in individuals with TBI, such as processing speed, working memory and new learning. Working memory was assessed with the Digit Span subtest of the Wechsler Adult Intelligence Scale (third edition), including simple attention/rehearsal (digits forward) and rehearsal/manipulation (digits backward; Wechlser, 1997). Processing speed, inhibition and cognitive set switching were assessed using the Trail-Making Test A and B (Reitan, 1958) and the Stroop Colour-Word test. Basic fund of knowledge was assessed using the Information subtest of the Wechsler Adult Intelligence Scale (third edition) (Wechlser, 1997).

Results

Demographics

Table 1 provides the mean and standard deviation for the two samples for demographic variables. The two samples were not significantly different in age, education or gender.

Behaviour

Table 2 provides the results of neuropsychological testing. The data are generally consistent with findings in TBI, where primary deficits in executive control and processing speed are evident. Of note, this sample of individuals with TBI showed milder impairments on tests of working memory outside the scanner.

Table 3 provides the results for performance on the *n*-back task during functional MRI data acquisition. Overall, individuals with TBI demonstrated diminished accuracy and reaction time during the 1-back and comparable reaction times during the 2-back tasks. When considering the entire sample, the influence of task load was observed for both accuracy and reaction time. Finally, early versus late effects on reaction times were observed in the TBI group for the 2-back condition.

Table 2 Neuropsychological test results for TBI and healthy control samples

Neuropsychological test	TBI, (mean, SD)	Healthy control (mean, SD)	Group comparison, *P*-value
Trail making test A	34 s, 8.98	21 s, 7.76	<0.001
Trail making test B	83 s, 35.06	50 s, 13.6	0.007
Stroop (colour-word)	88, 20.34	105, 11.30	0.03
Information (WAIS-III)	15.67, 7.01	20.7, 5.52	0.08
Digit Span (WAIS-III)	17.5, 11.36	19.27, 8.4	0.21

TBI = traumatic brain injury; WAIS-III = Wechsler Adult Intelligence Scale (third edition).

Table 3 Influence of group, task load and task exposure on accuracy (%) and reaction time (ms)

	Combined groups mean (SD)	TBI mean (SD)	Healthy control mean (SD)
Accuracy			
1-back	93 (13)*	86 (16)†	99.3 (1)†
2-back	86 (16)*	84 (16)	87.8 (16)
1-back early	91 (16)	84 (20)†	98.6 (3)†
1-back late	94 (11)	88 (13)†	100 (0)†
2-back early	84.7 (20)	82.8 (23)	89 (17)
2-back late	87.6 (14.6)	86 (12)	88 (16.5)
Reaction time			
1-back	663.6 (136.3)*	721.9 (100.0)†	605.3 (146.5)†
2-back	742.4 (170.1)*	773.6 (182.5)	711.2 (158.4)
1-back early	657.8 (134.4)	720.7 (135.3)†	594.9 (104.0)†
1-back late	669.5 (178.3)	723.1 (127.7)	615.8 (209.6)
2-back early	780.6 (188.4)**	821.9 (180.5)**	739.3 (194.7)
2-back late	704.3 (167.4)**	725.4 (191.3)**	683.2 (144.9)

*Within-group × load $P < 0.05$; **Within-group × time $P = 0.002$;
†Between-group comparison, $P < 0.05$.
TBI = traumatic brain injury.

Connectivity analysis

Examining connectivity frequency

In order to establish the between-time point changes in neural connectivity, separate extended-unified structural equation models were estimated for each individual at each half of each run. We estimated a total of four models per individual *via* the automatic search procedure. Again, all individual extended-unified structural equation models were subjected to rigorous statistical fit thresholds (root mean squared error of approximation <0.05, standardized root mean squared residual <0.05, comparative fit index >0.95, non-normed fit index >0.95), ensuring that the final model fits the data well. For confirmatory models, non-significant connections were not included. The final confirmatory

Table 4 Montreal Neurologic Institute (SPM5) *x*, *y*, *z* coordinates for peak values in each of the six regions of interest for both groups

TBI	*x*	*y*	*z*	HC	*x*	*y*	*z*
	Right prefrontal cortex				Right prefrontal cortex		
1-back	43.25 (6.8)	34.58 (8.8)	23.62 (7.4)	1-back	46.58 (8.6)	33.92 (8.7)	23.96 (27.6)
2-back	44.25 (8.1)	36.21 (8.5)	22.79 (7.2)	2-back	45.58 (5.7)	33.5 (8.9)	23.21 (6.2)
	Right anterior cingulate cortex				Right anterior cingulate cortex		
1-back	8.67 (4.6)	20.83 (8.7)	35.08 (12.2)	1-back	8.54 (4.9)	18.29 (8.8)	34.63 (10.1)
2-back	10.42 (3.5)	25 (8.8)	31.75 (12.7)	2-back	9.54 (5.9)	19.67 (7.9)	35.92 (9.9)
	Right parietal				Right parietal		
1-back	49.21 (10.9)	−42.12 (6.4)	38.96 (8.3)	1-back	51.67 (10.4)	−43.46 (12.0)	32.21 (10.3)
2-back	47.08 (10.7)	−41.38 (6.5)	36.38 (6.2)	2-back	49.13 (12.7)	−40.67 (11.1)	32.17 (18.9)
	Left prefrontal cortex				Left prefrontal cortex		
1-back	−41.08 (6.0)	30.67 (8.4)	24.25 (6.8)	1-back	−45.75 (6.4)	26.83 (10.7)	47.36 (6.1)
2-back	−43.5 (6.5)	33.08 (7.5)	22.71 (6.3)	2-back	−44 (6.0)	29.58 (10.7)	23.88 (6.7)
	Left anterior cingulate cortex				Left anterior cingulate cortex		
1-back	−6.33 (3.7)	17.42 (7.2)	40.29 (8.7)	1-back	−6.83 (4.0)	16.88 (5.3)	37.17 (9.9)
2-back	−7.9 (3.7)	18.29 (6.2)	37.5 (7.2)	2-back	−8.04 (5.9)	17.42 (7.0)	39.92 (6.2)
	Left parietal				Left parietal		
1-back	−43.42 (9.3)	−40.17 (17.1)	37.33 (7.8)	1-back	−50.58 (9.7)	−42.17 (7.9)	32.42 (11.1)
2-back	−39.5 (20.7)	−36.5 (24.6)	36.58 (8.7)	2-back	−49 (9.7)	−42.38 (8.3)	35.79 (10.2)

All peak values for each subject for each time series restricted to within the perimeter of the regions of interest taken from the Talairach Daemon. Prefrontal cortex is Brodmann area 46, anterior cingulated cortex is Brodmann area 32 and parietal lobe is Brodmann area 40.
HC = healthy control; TBI = traumatic brain injury.

models evidenced excellent fits: 97% met the stringent criteria for an excellent fit on at least one of the four fit indices above (root mean squared error of approximation, standardized root mean squared residual, non-normed fit index and comparative fit index) with the remaining 3% being considered acceptable fits by these indices. Thus the final models contain only connections that significantly predicted region of interest activity in that person for that run. This rigorous approach ensures that reliable estimates for each individual are obtained. The extended-unified structural equation model was applied to six region of interest time series for two groups of 12 subjects, resulting in 24 effective connectivity maps for each of the four factors of interest: 1-back early; 1-back late; 2-back early; and 2-back late. See Table 4 for the mean locations within each region of interest for each subject group.

As only significant connections are retained in the final extended-unified structural equation model maps, connections not estimated were considered to have a 'zero' for the β weight. A bimodal distribution thus occurs when looking at values for a path across individuals since those without the connection have zeros and those with the connection have normally distributed β weights. To examine the influence of group (i.e. healthy controls versus TBI) and time (i.e. early versus late) we aimed to focus on change in the frequency of connections as opposed to the strength of those connections. As noted above, this approach to data aggregation eliminates the possibility that group-level data include connections that do not exist in the individuals comprising that group. In doing so, the absolute values of the resulting β weights across individuals reveals a bimodal distribution so that for any two regions of interest for an individual, the connection between them is labelled either 1 (positive connection) or 0 (no connection).

Extended unified structural equation modelling: testing the hypotheses

To establish individual connectivity maps, binary connection values were based on findings that were highly reliable for each subject. In order to reduce the number of statistical comparisons, only analyses directly related to testing the hypotheses were conducted.

Right and left hemisphere connectivity

To examine the hypothesized role of the right hemisphere in initial task processing, we specifically examined the frequency of connections within the left hemisphere, within the right hemisphere and between-hemispheres. Three separate $2 \times 2 \times 2$ analyses of variance were conducted to examine the influence of group (between subjects), time and load (within subjects) on the frequency of connectivity. First, an ANOVA revealed a main effect of load for total number of connections (considering left and right hemispheres together) [F (1, 20) = 7.504, $P = 0.013$] (Fig. 1A). Second, an ANOVA was conducted to test the effects of group, time and load on connections within the left hemisphere, revealing a significant main effect of load, [F (1, 20) = 16.969, $P = 0.001$] and an interaction of load and time, [F (1, 20) = 4.343, $P = 0.05$] (Fig. 1C). Finally, an ANOVA was conducted to test the effects of group, time and load on connections within the right hemisphere, resulting in a nearly significant interaction of load, time and group [F (1, 20) = 3.271, $P = 0.086$] (Fig. 1D).

To test the hypotheses, *post hoc* t-tests were conducted examining the relationships between group, time and load and their influence on left and right hemisphere connectivity (only as

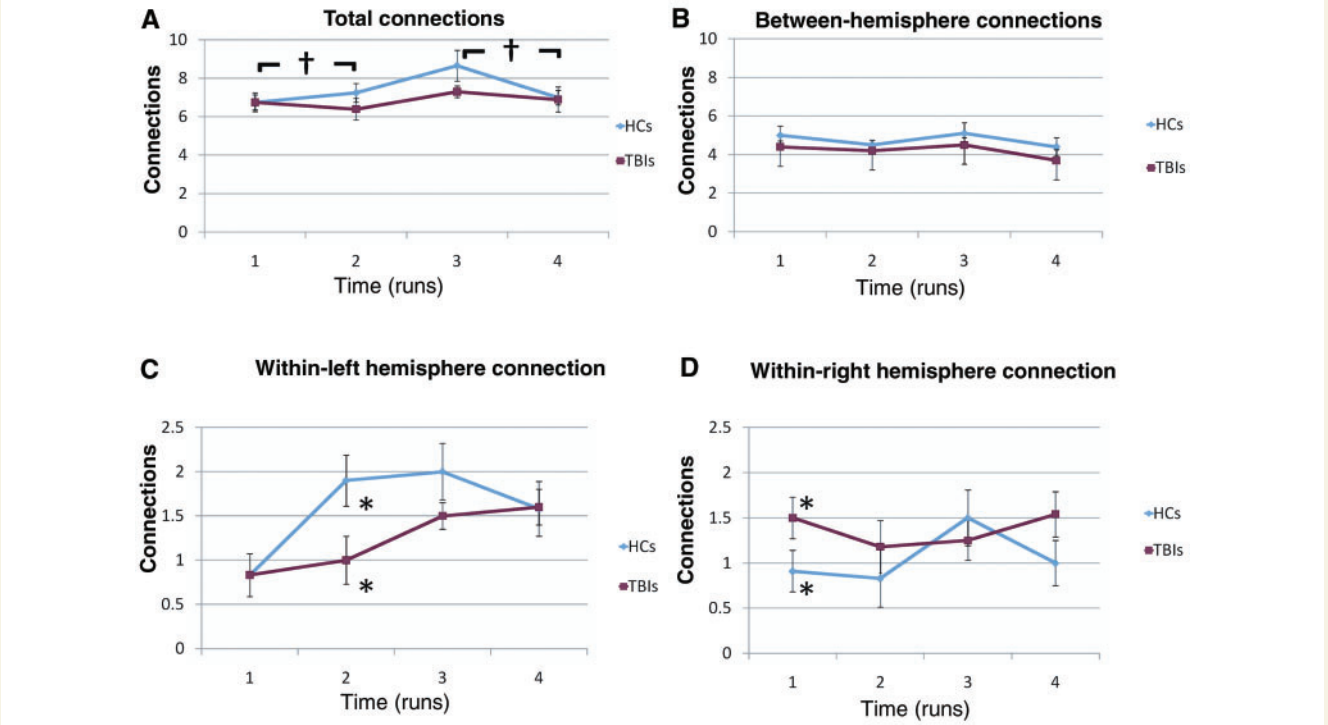

Figure 1 (**A–D**) Mean connectivity values (with standard error) for total connections and between- and within-hemisphere connections in both samples. Data collapsed for load. Run 1 = 1-back early, Run 2 = 1-back late, Run 3 = 2-back early, Run 4 = 2-back late; HC = healthy control; LPFC = left prefrontal cortex; RPFC = right prefrontal cortex; TBI = traumatic brain injury. $^{*}P < 0.05$ between groups, $^{\dagger}P < 0.05$ for load.

noted below, a one-tailed test was used for analyses specific to hypothesis and when the direction was predicted). To guide these statistical comparisons, first the data were plotted in group × time for the four time points (Fig. 1A–D). Based upon ANOVA result, there was a significant effect of load on total connectivity, with connections increasing with load (Fig. 1A), but as can be seen in Fig. 1A and B, there were no significant between-group differences in total connectivity (more on this below) or in between-hemisphere connectivity. When examining within-hemisphere connectivity, results did reveal that the TBI sample demonstrated greater within-right hemisphere connectivity early during the 1-back [frequency 1.50 in TBI versus 0.916 in healthy controls; t (22) = 1.79; $P = 0.043$, Cohen's $d = 0.74$; one-tailed], but a non-significant difference during the 2-back [frequency 1.5 in TBI versus 1.0 in healthy controls; t (21) = 1.56; $P = 0.065$, Cohen's $d = 0.64$; one-tailed]. The sample of healthy controls demonstrated significantly greater within-left hemisphere connectivity later in the 1-back [frequency 1.9167 in healthy controls; 1.00 in TBI; t (21) = –2.31; $P = 0.031$, Cohen's $d = -0.95$] (Fig. 1C and D). Consistent with this, when comparing each hemisphere, between-group results demonstrated that the sample of healthy controls was more left-lateralized than the TBI group late during the 1-back [−1.0833 in healthy controls versus 0.1818 in TBI; t (21) = 2.12; $P = 0.045$, Cohen's $d = -0.90$]. When examining only the TBI sample, within-left hemisphere connections did not significantly increase from early to late during the 1-back [frequency 0.81 to 1.0; t (10) = −0.516; $P = 0.61$] but this leftward shift was observable when examining early in the 1-back in TBI to both early in the 2-back [frequency 0.8333 to 1.5; t (11) = −2.34; $P = 0.039$; Cohen's $d = -0.97$] and late in the 2-back [frequency 0.72 to 1.63; t (11) = −4.30; $P = 0.002$; Cohen's $d = -1.25$]. Thus, the TBI sample maintained increased right hemisphere connectivity overall and was slower to demonstrate the growing left hemisphere connectivity observed in the sample of healthy controls.

Finally, correlational analyses between within-right and within-left hemisphere connectivity and task reaction time were conducted to determine the relationship with performance. To guarantee variance, these analyses focused on total within-hemisphere connectivity and change in reaction time. Pearson correlations revealed nearly significant relationships between reaction time change and change in within-right hemisphere connectivity during the 1-back ($r = -0.56$, $P = 0.071$) and 2-back ($r = -0.59$, $P = 0.056$) and a non-significant relationship between reaction time change and within-left connectivity change during the 1-back ($r = -0.296$, $P > 0.05$), but a significant relationship with change in left hemisphere during the 2-back ($r = -0.662$, $P = 0.027$). These data indicate that, when considering the entire right hemisphere, increased within-hemisphere connectivity is associated with decreased reaction times (improved performance), but that this effect may be load-dependent in the left hemisphere.

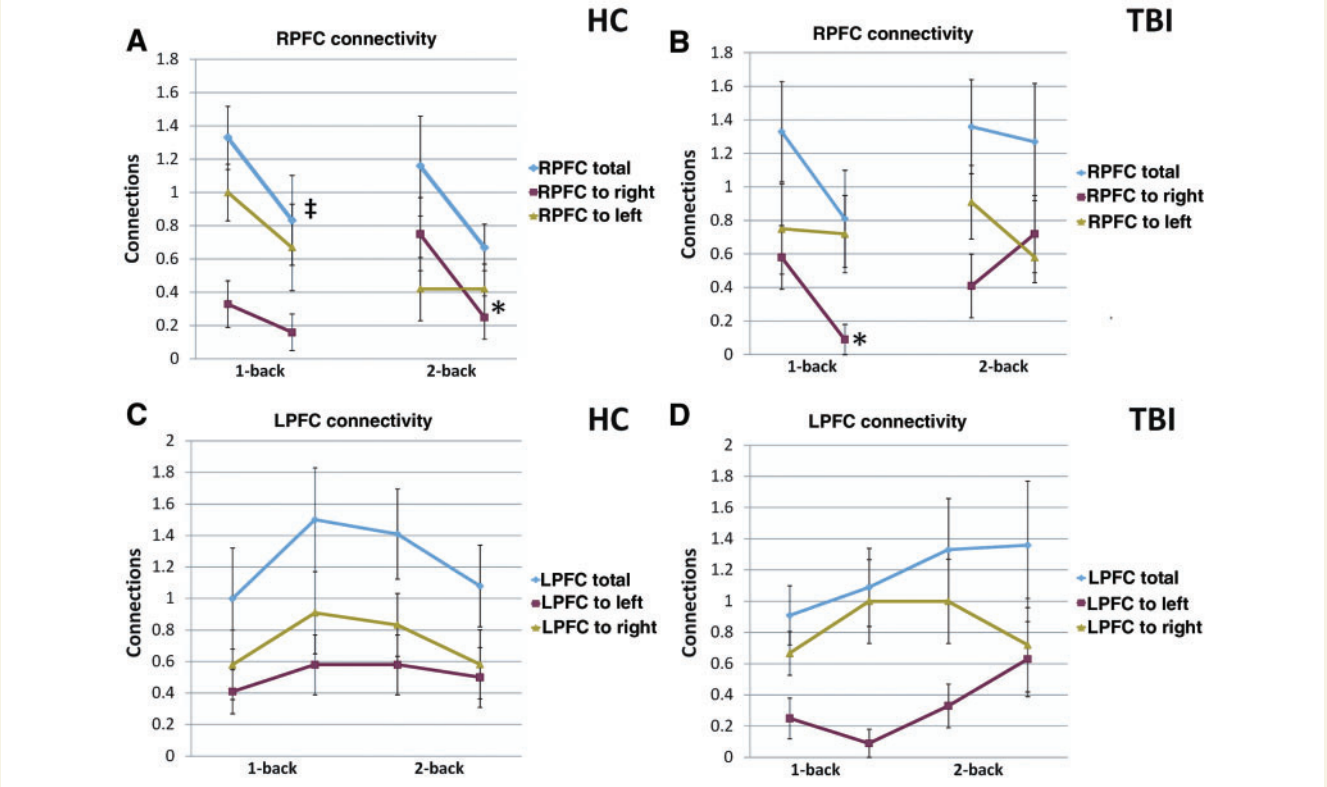

Figure 2 Mean connectivity values (with standard error) for total connections and between and within-hemisphere connections for right prefrontal cortex (RFPC) and left prefrontal cortex (LPFC) in both samples. HC = healthy control; TBI = traumatic brain injury. $^{*}P < 0.05$ within-sample effect of time; $^{\ddagger}P < 0.10$ within-sample effect of time.

Prefrontal cortex connections

To explore the role of prefrontal cortex in the hemisphere effects observed above, right and left prefrontal cortex connectivity were plotted for each of the four time points for: (i) total connections; (ii) connections with the left hemisphere; and (iii) connections within the right hemisphere.

Prefrontal cortex total connections

As can be seen in Fig. 2A–D, with respect to total right prefrontal cortex connectivity, the healthy controls sample reveals a downward shift at both loads, but the TBI mirrors this response only for the 1-back and shows no real change from early to late in the 2-back. In left prefrontal cortex, the healthy controls quickly reach asymptote by late in the 1-back and the TBI group continues to develop connections until late into the 2-back. Overall, the total number of connections for right prefrontal cortex shows a response pattern more closely linked to load and time and the left prefrontal cortex shows a response pattern more closely linked to time irrespective of load in both groups.

Within-hemisphere prefrontal cortex connections

Consistent with healthy controls, the TBI sample demonstrates a significant downward shift in right prefrontal cortex connectivity within the right hemisphere from early to late in the 1-back [frequency 0.58 to 0.09; t (10) = 1.83; $P = 0.048$; Cohen's $d = 0.85$], but there is an interaction of group × time for the 2-back where the healthy controls demonstrate a reduction in right prefrontal cortex from early to late during the 2-back, but inconsistent with Hypothesis 1b, the TBI sample demonstrates a non-significant increased right prefrontal cortex involvement from early to late in the 2-back. Consistent with what is observed in the 'within-left hemisphere' findings above, connections from left prefrontal cortex to the left hemisphere in the TBI group are late to develop and the healthy controls group has already plateaued and begun to decline by the late 2-back period (Fig. 2C and D).

Between-hemisphere prefrontal cortex connections

In the TBI sample, there is little change of connectivity from right prefrontal cortex to the left hemisphere during the 1-back, whereas the healthy controls showed a slight decrease to asymptote over time. Declining between-hemisphere connectivity appeared by the end of the 2-back in the TBI sample (Fig. 2A and B) and is consistent with the delayed development of connections within the left hemisphere. In left prefrontal cortex, between-hemisphere effects were nearly identical for both groups and responded to time irrespective of load (Fig. 2C and D). Finally, to examine the connectivity between the two prefrontal cortex regions, specifically, we examined the influence of right prefrontal cortex on left prefrontal cortex over time in the TBI sample (Hypotheses 1a and b). Two-tailed test results revealed a non-significant decline in right prefrontal cortex influence on left prefrontal cortex from early to late in the 1-back [frequency 0.27 to 0.18; t (11) = 1.0; $P = 0.34$] and a significant decline in this influence during the

2-back [frequency 0.45 to 0.09; $t(11) = 2.39$; $P = 0.02$; Cohen's $d = 0.848$].

Density of network connectivity

As noted, there was a main effect of task load on the total number of connections, with the network becoming denser as task load increased (total frequency 1-back: 1.0833; 2-back: 1.9167; $P = 0.035$). However, when examining the hypothesis regarding the total number of connections between groups, and from early to late, there were no significant differences. For example, when collapsing across task load (1-back and 2-back), there were no between-group differences in the total number of connections (healthy controls = 7.4167; TBI = 7.0250; $P = 0.372$). There was also no effect of task load on the total number of connections during between group comparisons: 1-back early (healthy controls = 6.75; TBI = 6.75; $P = 1.00$); 1-back late (healthy controls = 7.2500; TBI = 6.4545 $P = 0.298$); 2-back early (healthy controls = 8.6667; TBI = 7.3333; $P = 0.235$); 2-back late (healthy controls = 7.000; TBI = 6.9091; $P = 0.903$).

Anterior–posterior modulation

Finally, it was a goal to examine between-group differences and change in the connectivity between anterior and posterior network nodes. An independent sample *t*-test revealed that the parietal lobe influenced the frontal regions more in healthy controls than patients with TBI overall (healthy controls = 1.8958 versus patients with TBI = 1.4500; $P = 0.041$). In the TBI sample, the influence of the left parietal on the left prefrontal cortex ($P = 0.03$) and left anterior cingulate cortex ($P = 0.043$) increased from early to late 1-back. Furthermore, the influence of left parietal on left anterior cingulate cortex also increased from early to late during the 2-back ($P = 0.017$), so the increased influence of left parietal on left anterior cingulate cortex over time was consistent at both loads. Finally, there was a general load/time effect within the TBI sample, with greater parietal influence on the network from 1-back to 2-back.

Group frequency map

The analyses above demonstrate trends in overall connectivity across and within individuals. However, these analyses do not permit a representation of the connections most frequently occurring within the current data. Thus, it was also goal in the current application of the extended unified structural equation model to derive group-level effective connectivity maps based upon the frequency of observed connections to offer representative group images of connectivity changes. This approach retains the high resolution of the extended unified structural equation model to document individual connections, and does not average covariance matrices across individuals, which tends to produce misleading aggregate representations (cf. Molenaar, 2004). Figures 3–6 demonstrate network connectivity based on the frequency of observable connections. In order for any connection to be retained in the model, it was necessary for at least 40% of the sample to demonstrate that connection either 'early' or 'late' in the task for each task load (1-back and 2-back considered separately here). Because of this, these final analyses were distilled to only the most frequently observed connections in order to permit isolation of common group connection changes. Of critical importance, the influence of task 'input' was primarily observed in the left hemisphere in the healthy controls sample and in the right hemisphere in the TBI sample. Also, consistent with the hypotheses is the reduced influence of right prefrontal cortex from early to late for each task load in the TBI sample.

Discussion

The goal of this study was to examine effective network connectivity in individuals who have sustained severe TBI with focus on understanding how disrupted neural networks accommodate novel tasks. Thus, the goal was to understand how task acquisition (i.e. learning) occurs in a disrupted neural system with specific attention given to the interaction between relevant components within the network, as opposed to the magnitude of the response in the individual components (as observed in traditional topographical activation studies). In order to achieve this goal, we focused on network change while subjects were engaged in a well-established working-memory task (i.e. *n*-back). The analysis here focused on connection frequency as the basis for model building; an alternative and more conservative approach to traditional structural equation model methods that pool variance to arrive at a mean β-value for each connection. To the best of our knowledge, this is the first functional imaging study to examine cognitive plasticity after neurological compromise using connectivity modelling and the first to employ these advanced connectivity methods (i.e. extended-unified structural equation model; Gates *et al*., 2010*a, b*).

Primary findings

In testing the first Hypotheses (1a and b), it was a goal to determine if the right hemisphere plays a unique role in task acquisition after TBI. We anticipated that, compared to the healthy controls sample, individuals sustaining TBI would demonstrate greater right hemisphere influence on the network (with emphasis on the right prefrontal cortex) and this hypothesis was based on the observation in traditional 'activation' studies that right prefrontal cortex may be differentially recruited in TBI samples during tasks of working memory (McAllister *et al*., 1999, 2001; Christodoulou *et al*., 2001; Perlstein *et al*., 2004; Maruishi *et al*., 2007; Hillary *et al*., 2010). As noted, one interpretation of this neural recruitment is that it represents increased allocation of cognitive control resources to permit the development of task routines during task acquisition (Hillary, 2008). Thus, as a corollary to Hypothesis 1a, we anticipated that as task exposure increased, the demand for greater cognitive control oversight in TBI should diminish (Hypothesis 1b). We anticipated that this effect would be observed in the current data as increased connectivity between right prefrontal cortex and other nodes within the network early during task engagement and that this effect should diminish over time as task subroutines are developed. In order to examine this position we analysed average frequencies derived from

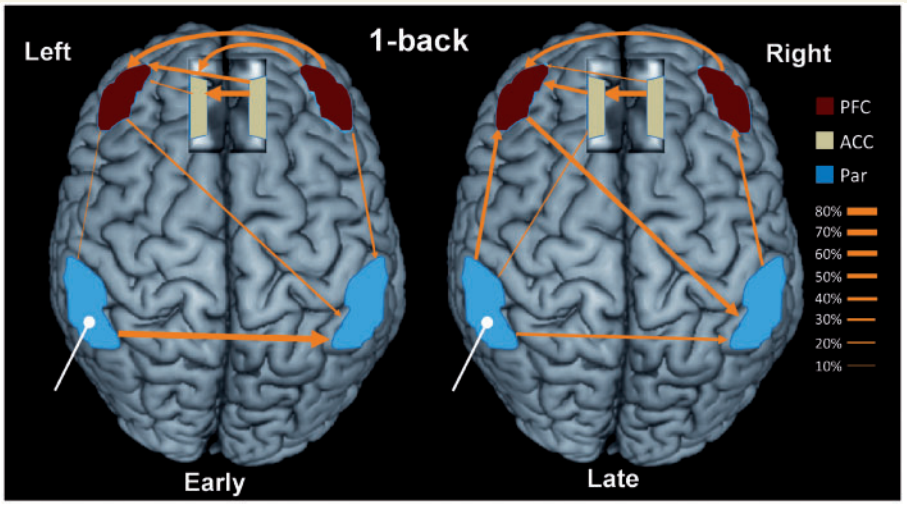

Figure 3 Group frequency data for effective connectivity in the healthy control sample for 'early' and 'late' effects during the 1-back. Line thickness indicates frequency of connections. The primary influence of 'task input' is represented as a white bar. Coloured Brodmann areas are a schematic representation illustrating the approximate spatial constraints for the regions of interest (i.e. peak + 5 mm sphere). ACC = anterior cingulate cortex; Par = parietal; PFC = prefrontal cortex.

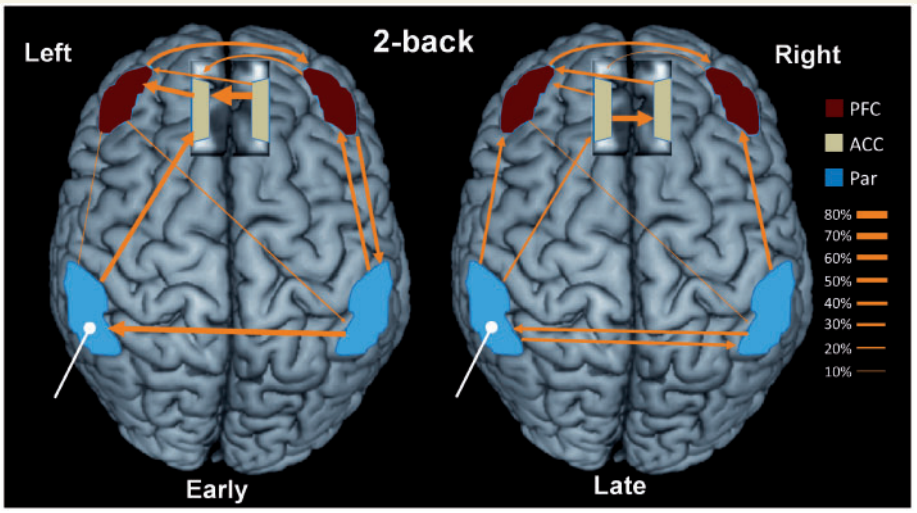

Figure 4 Group frequency data for effective connectivity in the healthy control sample for 'early' and 'late' effects during the 2-back. Line thickness indicates frequency of connections. The primary influence of 'task input' is represented as a white bar. Coloured Brodmann areas are a schematic representation illustrating the approximate spatial constraints for the regions of interest (i.e. peak + 5 mm sphere). ACC = anterior cingulate cortex; Par = parietal; PFC = prefrontal cortex.

individual extended unified structural equation model models (Figs 1 and 2) as well as qualitative analysis of group data based on the most frequently observed connections (Figs 3–6). Each of these analyses lent support to the hypotheses and is discussed in turn below.

Examining within- and between-hemisphere connectivity

The most consistent intra-hemispheric findings observed in the frequency data were that the TBI sample demonstrated consistently elevated within-right hemisphere connectivity and a protracted leftward shift in connections compared to the healthy controls sample. These general effects in the left hemisphere also served as the blueprint for the evolution of left prefrontal cortex connections in TBI. The elevated right hemisphere involvement in TBI compared to healthy controls (Figs 1D, 2A and B) represented a combination of both right prefrontal cortex effects (early decreases during 1-back and increases from early to late 2-back) and right parietal effects that increase within each task load, with the net result reflecting greater involvement in TBI.

When juxtaposing the two patterns of altered connectivity observed in right and left prefrontal cortex, what emerges is the

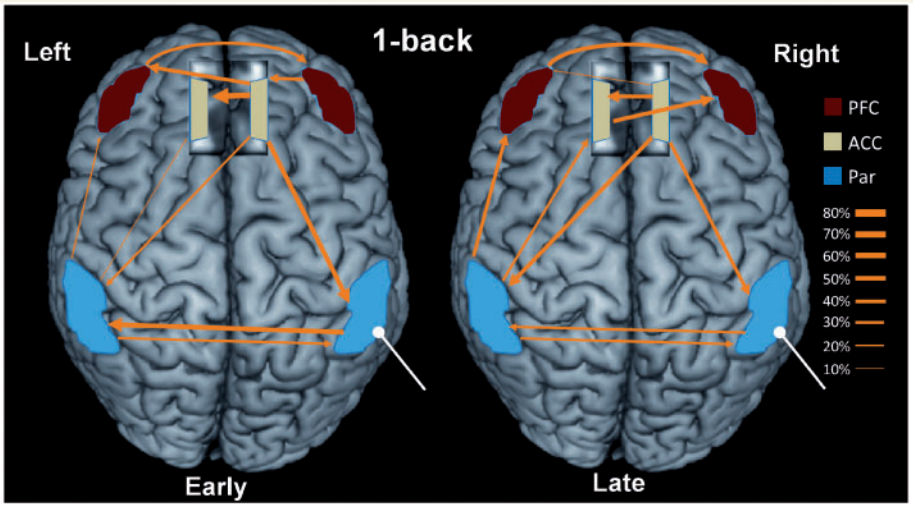

Figure 5 Group frequency data for effective connectivity in the traumatic brain injury sample for 'early' and 'late' effects during the 1-back. Line thickness indicates frequency of connections. The primary influence of 'task input' is represented as a white bar. Coloured Brodmann areas are a schematic representation illustrating the approximate spatial constraints for the regions of interest (i.e. peak + 5 mm sphere). ACC = anterior cingulate cortex; Par = parietal; PFC = prefrontal cortex.

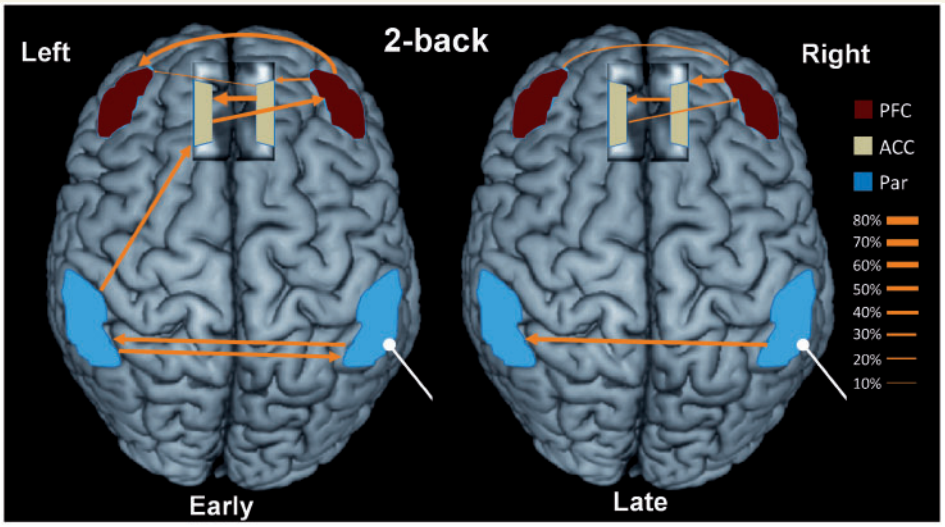

Figure 6 Group frequency data for effective connectivity in the traumatic brain injury sample for 'early' and 'late' effects during the 2-back. Line thickness indicates frequency of connections. The primary influence of 'task input' is represented as a white bar. Coloured Brodmann areas are a schematic representation illustrating the approximate spatial constraints for the regions of interest (i.e. peak + 5 mm sphere). ACC = anterior cingulate cortex; Par = parietal; PFC = prefrontal cortex.

differential effects of load and time for connectivity. Right prefrontal cortex appears to be more responsive to task load (with time influencing connections within each load level) while left prefrontal cortex connections appear here to respond primarily to time on task (irrespective of load). This effect is clearer in the healthy controls sample (Fig. 2A and C); as the task formalizes in the healthy controls sample over time, left prefrontal cortex increases to asymptote and then declines and right prefrontal cortex shows sharp decline while responding to each load. In the TBI sample, there is a latency in left hemisphere connectivity so that by late in the 2-back, the total number of connections reaches the point where the healthy controls sample peaked late in the 1-back (time being the critical determinant). In the right prefrontal cortex, however, connectivity is tied to task load, but with some inconsistency in the direction of recruitment, including diminishing connections from early to late in the 1-back and relatively constant connections in the 2-back (Fig. 2A and B). This latest finding is inconsistent with Hypothesis 1b and may be attributable to a shift in the connections between- and within-hemisphere. That is, right prefrontal cortex influence on the left hemisphere (and left

prefrontal cortex specifically) appears to decline, but its within-hemisphere influence is increasing and may be partially due to the increased parietal connectivity observed over time.

Overall, we interpret these laterality effects observed between groups to be the result of more persistent task 'novelty' in the TBI sample relative to healthy controls resulting in greater right hemisphere influence in TBI and a rapid 'leftward' shift in the healthy controls sample as task procedures are more readily formalized (Fig. 1C). These data are generally consistent with what would be expected if the role of increased right prefrontal cortex involvement after neurological disruption represents increased allocation of cognitive control resources during periods of inefficiency or as novel task demands are accommodated (Kelly *et al*., 2006). This finding is most evident during very early task acquisition (i.e. early to late in the 1-back) where right prefrontal cortex decline is significant. The distinct effects observed in the 2-back may reflect a renewed demand on cognitive control resources with increased task load. Even so, there is general support here for relatively greater influence of right prefrontal cortex after head injury and a potentially unique role for right prefrontal cortex in handling task novelty early on so that task routines can be more concretely formalized in left hemisphere (Gazzaniga, 2000).

Whole-brain connectivity

Based on our earlier work examining recovery after TBI (Nakamura *et al*., 2009), we anticipated that the total number of connections within the nodes represented here would be greater in TBI compared to healthy controls and that this number of connections would be task load sensitive and decline over the course of the task (Hypothesis 2). While there was a main effect of task load (1-back to 2-back) on connections, with the total number increasing with load, in general this hypothesis was not supported. There are likely to be two important reasons why between-group differences were not observed here. First, the findings by Nakamura *et al*. (2009) were based on a measure of non-task related connectivity and the specific relationships between resting and stimulus-related networks remain an emerging area of investigation in the clinical neurosciences. Secondly, the data in this earlier study (Nakamura *et al*., 2009) included 112 distinct regions of interest without focus on specific working-memory networks compared to the six (bilateral) regions of interest examined in the current study. Because the extended-unified structural equation model is a novel technique, we chose to examine a well-established task and substrates commonly linked to working memory to constrain the analyses and hypotheses. However, inclusion of a greater number of regions of interest would afford the opportunity to observe any expansion or pruning of secondary support connections and to document global connectivity change. Whatever the reason, the current data did not offer evidence that healthy controls and TBI differ in the total number of connections early during task performance or later during task acquisition. This is not consistent with other work conducting partial correlation analysis to examine covariance between regions showing activation changes during new learning (Strangman *et al*., 2009) and is certainly an area requiring further inquiry using a larger number of task-related regions of interest. Of note, the frequency distribution does indicate that individuals with TBI may show a greater number of 'highly frequent' connections, which may be a starting point for further analyses examining network sparsity. Even so, overall these data indicate that within this discrete group of network nodes, the overall loss or gain in connections due to injury is negligible.

Anterior and posterior network influence

Finally, we hypothesized that there would be a shift from anterior to posterior influence to posterior to anterior influence as the primary load on attentional control in prefrontal cortex/anterior cingulate cortex diminished and task formalization resulted in spatial/sensory representation of the task (Hypothesis 3). Findings revealed greater parietal influence on anterior networks in the healthy controls sample compared to individuals with TBI. The injured group demonstrated consistent effects for both task loads; task exposure in the TBI sample resulted in decreased anterior involvement relative to parietal control, resulting in an anterior to posterior 'shift'.

Thus, the observable shift in network emphasis from anterior to posterior for all three of these findings in TBI (e.g. early versus late 1-back; early versus late 2-back; 1-back versus 2-back) can all be attributable to changes associated with task exposure. While the current data clearly demonstrate a shift in influence from anterior to posterior over time in TBI, additional work is needed to differentiate the effects of task load and performance change on anterior and posterior network influence.

Group data: isolating the most consistent connections

A second approach to examining the current data was to generate group level connection maps to examine the most frequently observed connection changes in each group. The most striking finding from these group connectivity analyses was that during both task loads of the *n*-back, the 'input', or influence of task, was most commonly associated with right parietal influence in the TBI sample and left parietal influence in the healthy controls sample (Figs 3–6). This hemispheric difference in the expression of task input can be interpreted to mean that network variance at the outset of task processing is more highly influenced by the right hemisphere in the TBI group compared to predominantly left hemisphere influence in the healthy controls sample. With some variability, these models also support Hypothesis 1b; right prefrontal cortex influence diminishes with time for both loads. These findings reveal the most consistently observed connections in the data set and support the view that the right hemisphere is differentially engaged after neurological disruption and we attribute this to slowed task proceduralization and continued demand on cognitive control resources during task acquisition.

Implications for understanding neural plasticity in traumatic brain injury

The current study provides several insights into how large-scale neural networks adapt to a novel task. Of note, this group of individuals sustained significant, unequivocal neurological disruption, where at least 67% had verifiable injury to frontal systems and 85% included frontal and/or parietal injury. It was also the case that individuals in this sample maintained adequate working memory functioning and were able to perform the task, which is essential for examining residual cognitive capacity using functional imaging methods (Price and Friston 2002; Price *et al.*, 2006). Thus, the current approach affords the opportunity to examine how disrupted neural networks accommodate novel tasks over time, or—in other words—how they 'learn'.

These data illustrate how disrupted networks accommodate novel tasks in two important ways. First, it should be noted that the task-related topographical activation in these data was consistent with a larger literature; individuals with TBI demonstrated expansion of task-related activity in right prefrontal cortex in the context of significantly impaired performance during the 1-back. Moreover, the between-group differences in right prefrontal cortex during the 2-back was attenuated and this corresponded to no performance differences between the groups (for complete results see Medaglia *et al.*, in press). However, total right prefrontal cortex connectivity remained elevated late into the 2-back (compared to healthy controls) and its differential influence on left prefrontal cortex (diminished) and the right hemisphere (increased) cannot be observed when examining the topographical activation alone. A tacit assumption in topographical activation studies that focus on the magnitude of BOLD signal change is that the components within the network at any given time point (or between two groups) are operating identically, including any possible direction of influence and strength of network connections. Such an assumption is not sustainable if functional imaging methods are to continue to advance our understanding of brain-behaviour relationships and the current approach offers initial insights into how one might think beyond topography and to integration.

A second observation to be made from these data is that disrupted networks remain highly fluid and show connectivity changes in a short period of time (i.e. within a run). We observe very clear maturational effects in connections, even for a 'simple' task like the 1-back. The short-term flexibility observed here is a key consideration given the gross signal averaging that imaging methods often require. Related to this, connections may respond differentially to the influences of time and load and may have distinct (or even no direct) consequences for task performance. For example, there appears to be greater influence of load on right prefrontal cortex connectivity within the right hemisphere, yet parietal connectivity within the same hemisphere shows incremental increases irrespective of load. In sum, much work is required to understand how the nodes within highly malleable networks interact in order to adapt to injury and permit new learning. The extended-unified structural equation model approach used here offers additional information about the nature of connectivity after neurological disruption that may be used in concert with topographical activation findings to examine recovery in dynamic neural systems.

Study limitations and future directions

While the current study offers the first application of a well-known cognitive task in the study of network disruption after TBI, there are noteworthy limitations that require acknowledgement. First, even with the focus on within-subject change and network connectivity in the individual, the sample size remains modest for a functional MRI study. While the connectivity analyses employed in this study are labour intensive, larger samples in the future will permit examination of the potential influences of demographic and factors (e.g. age, duration of coma) and clinical interventions on connectivity change after injury. Of note, however, between-group differences and early versus late changes in effective connectivity were large enough to be observable at this modest sample size, speaking to the robustness of the effects observed here. Related to this point, there were a number of *post hoc* statistical tests to examine network change and we did not employ statistical correction for each 'family' of analyses. There were a number of reasons for this. First, the final models derived by the extended-unified structural equation model represented a conservative estimation of network connections and, with this rigorous first level analysis in place, it was important to afford sensitivity to all observable effects (e.g. between-group, task load). Moreover, given the number of statistically significant findings observed, the overwhelming consistency in those findings, and that each test was conducted to test a specific hypotheses, it is highly unlikely that the results observed here are the result of statistical artefact.

One consistent concern when examining the effects of severe TBI is the influence of injury heterogeneity on group-level analyses and the potential influences of the injury on the BOLD signal. As noted, the most dependable finding in the functional imaging literature examining cognitive deficit in TBI is the observation that prefrontal cortex shows greater engagement and this has been observed despite the vast heterogeneity that is endemic to the disorder. This suggests that the dorsolateral prefrontal cortex 'recruitment effect' in particular is not explained by local influences on the BOLD signal. That is, if the BOLD signal is altered after injury, we anticipate that this disruption would not differentially influence the signal over the course of the task and certainly not in the hypothesized direction. Moreover, in the case of heterogeneous injury findings, we anticipate that distinct lesion constellations in subjects comprising the TBI sample would make it more and not less difficult to garner consistent results and test these hypotheses. For these reasons, we anticipate that the current findings are not a product of injury heterogeneity or directly attributable to any specific pathophysiology.

Finally, future work requires examination of an extended neural network over time including other components of the working memory network (e.g. cerebellum). The regions of interest chosen for this study were based upon prior findings in the working memory literature examining TBI, but certainly working memory cannot be isolated to these regions (e.g. cerebellum).

Further work should examine within-subject change in an expanded network during in order to develop useful heuristics for how plasticity is expressed in the disrupted neural system.

Funding

New Jersey Commission on Brain Injury Research, Grant #: 0120090178; Pennsylvania Tobacco Settlement Funds; Social Sciences Research Institute, PSU, University Park.

References

Ashburner J, Friston K. Multimodal image coregistration and partitioning—a unified framework. Neuroimage 1997; 6: 209–17.

Brett M. The MNI brain and the Talairach atlas. Available from MRC CBU Imaging Wiki: http://imaging.mrc-cbu.cam.ac.uk/imaging/MniTalairach; 1999 (8 August 2010, date last accessed).

Brown TA. Confirmatory factor analysis for applied research. New York: Guilford Press; 2006.

Chang L, Speck O, Miller EN, Braun J, Jovicich J, Koch C, et al. Neural correlates of attention and working memory deficits in HIV patients. Neurology 2001; 57: 1001–7.

Christodoulou C, DeLuca J, Ricker JH, Madigan NK, Bly BM, Lange, et al. Functional magnetic resonance imaging of working memory impairment after traumatic brain injury. J Neurol Neurosurg Psychiatry 2001; 71: 161–8.

Friston KJ, Holmes AP, Poline JB, Grasby PJ, Williams SC, Frackowiak RS, et al. Analysis of fMRI time-series revisited. Neuroimage 1995; 2: 45–53.

Friston KJ, Jezzard P, Turner R. Analysis of functional MRI time-series. Hum Brain Mapp 1994; 1: 153–71.

Gates KM, Molenaar PCM, Hillary FG, Ram N, Rovine M. Automatic search for fMRI connectivity mapping: an alternative to Granger causality testing using formal equivalences among SEM path modeling, VAR, and unified SEM. Neuroimage 2010a; 50: 1118–25.

Gates KM, Molenaar PCM, Hillary FG, Slobounov S. Extended unified SEM approach for modeling event-related fMRI data. Neuroimage 2010b; 54: 1151–8.

Gazzaniga MS. Cerebral specialization and interhemispheric communication: does the corpus callosum enable the human condition? Brain 2000; 123: 1293–326.

Hart TJ, Whyte J, Kim J, Vaccaro M. Executive function and self-awareness of 'real-world' behavior and attention deficits following traumatic brain injury. J Head Trauma Rehabil 2005; 20: 333–47.

Hillary FG, Moelter ST, Schatz P, Chute DL. Seatbelts contribute to location of lesion in moderate to severe closed head trauma. Arch Clin Neuropsychol 2001; 16: 171–81.

Hillary FG. Neuroimaging of working memory dysfunction and the dilemma with brain reorganization hypotheses. J Int Neuropsychol Soc 2008; 14: 526–34.

Hillary FG, Genova HM, Chiaravalloti ND, Rypma B, DeLuca J. Prefrontal modulation of working memory performance in brain injury and disease. Hum Brain Mapp 2006; 27: 837–47.

Hillary FG, Genova HM, Medaglia JD, Fitzpatrick NM, Chiou KS, Wardecker BM, et al. The nature of processing speed deficits in traumatic brain injury: is less brain more? Brain Imaging Behav 2010; 4: 141–54.

Kim J, Zhu W, Chang L, Bentler PM, Ernst T. Unified structural equation modeling approach for the analysis of multisubject, multivariate functional MRI data. Hum Brain Mapp 2007; 28: 85–93.

Kelly C, Foxe JJ, Garavan H. Patterns of normal human brain plasticity after practice and their implications for neurorehabilitation. Arch Phys Med Rehabil 2006; 87 (Suppl 2): S20–9.

Langlois JA, Rutland-Brown W, Thomas KE. Traumatic brain injury in the United States: emergency department visits, hospitalizations, and deaths. Atlanta, GA: Centers for Disease Control and Prevention, National Center for Injury Prevention and Control; 2004.

Levine B, Cabeza R, McIntosh AR, Black SE, Grady CL, Stuss DT. Functional reorganisation of memory after traumatic brain injury: a study with H2150 positron emission tomography. J Neurol Neurosurg Psychiat 2002; 73: 173–81.

Maguire EA, Vargha-Khadem F, Mishkin M. The effects of bilateral hippocampal damage on fMRI regional activations and interactions during memory retrieval. Brain 2001; 124: 1156–70.

Maruishi M, Miyatani M, Nakao T, Muranaka H. Compensatory cortical activation during performance of an attention task by patients with diffuse axonal injury: a functional magnetic resonance imaging study. J Neurol Neurosurg Psychiat 2007; 78: 168–73.

McAllister TW, Saykin AJ, Flashman LA, Sparling MB, Johnson SC, Guerin SJ, et al. Brain activation during working memory 1 month after mild traumatic brain injury: a functional MRI study. Neurology 1999; 53: 1300–8.

McAllister TW, Sparling MB, Flashman LA, Guerin SJ, Mamourian AC, Saykin AJ. Differential working memory load effects after mild traumatic brain injury. Neuroimage 2001; 1004–12.

McIntosh AR, Gonzalez-Lima F. Structural equation modeling and its application to network analysis in functional brain imaging. Hum Brain Mapp 1994; 2: 2–22.

Medaglia JD, Chiou KS, Slocomb J, Fitzpatrick NM, Ramanathan D, Vesek J, et al. The less BOLD, the wiser: support for latent resource hypothesis after neurotrauma. Hum Brain Mapp 12/10, in press.

Molenaar PCM. A manifesto on psychology as an idiographic science: bringing the person back into scientific psychology, this time forever. Measurement 2004; 2: 201–18.

Nakamura T, Hillary FG, Biswal BB. Resting network plasticity following brain injury. PLoS ONE 2009; 4: e8220.

Newsome MR, Scheibel RS, Hunter JV, Wang ZJ, Chu Z, Li X, et al. Working memory brain activation following severe traumatic brain injury. Cortex 2007; 43: 95–111.

Oikonomou VP, Tripoliti EE, Fotiadis DI. Bayesian methods for FMRI time-series analysis using a nonstationary model for the noise. IEEE Trans Inf Technol Biomed 2010; 14: 664–74.

Pardo JV, Fox PT, Raichle ME. Localization of a human system for sustained attention by positron emission tomography. Nature 1991; 349: 61–4.

Perlstein WM, Cole MA, Demery JA, Seignoural PJ, Dixit NK, Lason MJ, et al. Parametric manipulatio n of working memory load in traumatic brain injury: behavioral and neural correlates. J Int Neuropsychol Soc 2004; 10: 724–41.

Price CJ, Crinion J, Friston KJ. Design and analysis of fMRI studies with neurologically impaired patients. J Magn Reson Imaging 2006; 23: 816–26.

Price CJ, Friston KJ. 'Functional imaging studies of neuropsychological patients: applications and limitations. Neurocase 2002; 8: 345–54.

Reitan R. Validity of the Trail Making Test as an indicator of organic brain damage. Percept Motor Skill 1958; 8: 271–6.

Ricker JH, Muller RA, Zafonte RD, Black KM, Millis SR, Chugani H. Verbal recall and recognition following traumatic brain injury: a [0-15]-water positron emission tomography study. J Clin Exp Neuropsychol 2001; 23: 196–206.

Sanchez-Carrion R, Fernandez-Espejo D, Junque C, Falcon C, Bargallo N, Roig T, et al. A longitudinal fMRI study of working memory in severe TBI patients with diffuse axonal injury. Neuroimage 2008; 43: 421–9.

Sanchez-Carrion R, Gomez PV, Junque C, Fernandez-Espejo D, Falcon C, Bargallo N, et al. Frontal hypoactivation on functional magnetic resonance imaging in working memory after severe diffuse traumatic brain injury. J Neurotrauma 2008; 25: 479–94.

Sarty GE. Computing brain activity maps from fMRI time-series images. Canada: University of Saskatchewan; 2006.

Scheibel RS, Newsome MR, Steinberg JL, Pearson DA, Rauch RA, Mao H, et al. Altered brain activation during cognitive control in

patients with moderate to severe traumatic brain injury. Neurorehabil Neural Repair 2007; 21: 36–45.

Scheibel RS, Newsome MR, Troyanskaya M, Steinberg JL, Goldstein FC, Mao H, et al. Effects of severity of traumatic brain injury and brain reserve on cognitive-control related brain activation. J Neurotrauma 2009; 26: 1447–61.

Speck O, Ernst T, Braun J, Koch C, Miller E, Chang L. Gender differences in the functional organization of the brain for working memory. Neuroreport 2000; 11: 2581–5.

Strangman GE, Goldstein R, O'Neil-Pirozzi TM, Kelkar K, Supelana C, Burke D, et al. Neurophysiological alterations during strategy-based verbal learning in traumatic brain injury. Neurorehabil Neural Repair 2009; 23: 226–36.

Teasdale G, Jennett B. 'Assessment of command impaired consciousness: a practical scale. Lancet 1974; 304: 81–4.

Turner GR, Levine B. Augmented neural activity during executive control processing following diffuse axonal injury. Neurology 2008; 71: 812–8.

Wechlser D. Digit Span Subtest. WAIS-III Administration and Scoring Manual. San Antonio, TX: The Psychological Corporation; 1997a.

Wechlser D. Information Subtest. WAIS-III Administration and Scoring Manual. San Antonio, TX: The Psychological Corporation; 1997b.

Worsley KJ, Poline JB. Tests for distributed, nonfocal brain activations. Neuroimage 1995; 2: 183–94.